New similarity reductions and exact solutions for helically symmetric viscous flows

Cite as: Phys. Fluids **32**, 053604 (2020); https://doi.org/10.1063/5.0005423
Submitted: 02 March 2020 . Accepted: 20 April 2020 . Published Online: 12 May 2020

Dominik Dierkes, Martin Oberlack, and Alexei Cheviakov

New similarity reductions and exact solutions for helically symmetric viscous flows

Cite as: Phys. Fluids 32, 053604 (2020); doi: 10.1063/5.0005423
Submitted: 2 March 2020 • Accepted: 20 April 2020 •
Published Online: 12 May 2020

View Online Export Citation CrossMark

Dominik Dierkes,[1] Martin Oberlack,[1,a)] and Alexei Cheviakov[2]

AFFILIATIONS

[1] Chair of Fluid Dynamics, Department of Mechanical Engineering, Technische Universität Darmstadt, Otto-Berndt-Strasse 2, 64287 Darmstadt, Germany and Centre for Computational Engineering, Technische Universität Darmstadt, Dolivostraße 15, 64293 Darmstadt, Germany

[2] Department of Mathematics and Statistics, University of Saskatchewan, 106 Wiggins Road, Saskatoon, Saskatchewan S7N 5E6, Canada

[a)] **Author to whom correspondence should be addressed:** oberlack@fdy.tu-darmstadt.de

ABSTRACT

In the present paper, we derive exact solutions for the helically invariant Navier–Stokes equations. The approach is based on an invariant solution ansatz emerging from the Galilean group in helical coordinates, which leads to linear functions in the helical coordinate $\xi = az + b\varphi$ for the two helical velocity components u^ξ and u^η. The variables z and φ are the usual cylinder coordinates. Starting from this approach, we derive a new equation for the radial velocity component u^r in the helical frame, for which we found two special solutions. Moreover, we present an exact linearization of the Navier–Stokes equations by seeking exact solutions in the form of Beltrami flows. Using separation of variables, we found exponentially decaying time-dependent solutions, which consist of trigonometric functions in the helical coordinate ξ and of confluent Heun-type functions in the radial direction.

I. INTRODUCTION

Helical flow structures appear in various natural phenomena and technological devices, for example, in the wake of windmills,[1] as wing tip vortices,[2] in astrophysical plasmas (see, e.g., Ref. 3), and in laboratory applications, including "straight tokamak" plasma flow approximations (see, e.g., Refs. 4 and 5) and other experiments. In particular, helical vortex structures were observed by Sarpkaya[6] in experiments with swirling flows in a cylindrical tube, and as such, they are part of the various flow structures observed in the known vortex breakdown.

Various groups have worked on the theoretical description of helical flows in recent decades. The simplest approach here is to introduce a helical coordinate $\xi = az + b\varphi$, a, b = const $\neq 0$, where z and φ are the cylinder coordinates, and to assume that all physical quantities depend on the cylinder radius r and the helical coordinate ξ. Helically invariant flows include translationally and axially invariant ones as special cases. For the steady Euler equations describing incompressible fluid flows and for plasma equilibrium equations in the magnetohydrodynamics (MHD) framework, the helical invariance requirement allows us to reduce the governing equations to a single partial differential equation (PDE) known as the Johnson-Frieman-Kulsrud-Oberman (JFKO) equation.[5] This important equation generalizes the famous Bragg–Hawthorne–Grad–Rubin–Shafranov equation[7–9] describing steady axisymmetric inviscid flows onto the helically invariant case. Families of exact solutions of JFKO equations are known, including those derived by Bogoyavlenskij[3] (see also Refs. 10 and 11). In the more general context of helical geometry, several works focused on twisted pipes following a given spatial curve.[12–15] Using non-orthogonal and local-orthogonal coordinate systems, the effects of pipe curvature and torsion on the flow were investigated. Special analytical solutions of steady flows in helically symmetric pipes were found by Zabielski and Mestel.[16] For non-stationary helical flows, analytical solutions were derived by Ershkov (see Refs. 17 and 18). Delbende *et al.*[19] developed a direct numerical simulation (DNS) code for the helical invariant Navier–Stokes equations in a generalized vorticity-streamfunction formulation. Dritschel[20] reduced the three-dimensional (3D) Euler equations to a linear equation, assuming that the flow has a helical symmetry and consists of a rigidly rotating basic part and a Beltrami disturbance part. Furthermore, he derived exact solutions for flows in a straight pipe of circular cross section. Exact solutions for helical flows of a Maxwell fluid constrained between two infinite coaxial circular cylinders were derived by Jamil and Fetecau.[21]

While no general solution is available for the full time-dependent nonlinear PDE system of Navier–Stokes equations, multiple families of exact and approximate solutions describing specific situations have been derived. Well-known examples of solutions of incompressible Navier–Stokes equations in primitive variables include the Couette flow and the Hagen–Poiseuille flow in a cylindrical pipe. Among the most famous solutions for the Navier–Stokes equations in vorticity formulation are axisymmetric vortex-type solutions, such as the Oseen–Lamb vortex and the Taylor vortex, which describe columnar vortices without axial stretching. An example of exact solutions of axisymmetric flows containing axial vortex stretching is the famous Burgers vortex, which is the first stretched vortex solution that models turbulent eddies.[22]

A significant number of exact solutions of Navier–Stokes equations and related models, as well as of other nonlinear PDEs, have been derived in recent years with the help of techniques based on Lie groups, including local and nonlocal symmetries of PDEs, symmetry-invariant and partially invariant solutions, and their generalizations (see, e.g., Refs. 23–28 and references therein). For example, in Ibragimov,[23] several classes of invariant solutions of the Navier–Stokes equations are presented; in many cases, these solutions can be reduced to previously known solutions by choosing appropriate parameters. In Andreev *et al.*,[24] invariants of the Navier–Stokes equations in cylindrical coordinates were used to derive a system of ordinary differential equations (ODEs), for which exact solutions were obtained. In Sec. III A, we employ a similar approach to construct exact helically invariant solutions of Navier–Stokes equations.

Moreover, in Kumar and Kumar,[29] the strength of Lie group theory to construct exact solutions is shown for the steady state incompressible Navier–Stokes equations in two dimensions. The authors derived seven similarity solutions, using Lie point transformations, of which three are completely new. In all solutions, the contained singularities can be removed by setting certain parameters to zero and, in one of these solutions, the Reynolds number *Re* to infinity. This implies that for flows with a high *Re*-number, the inertial terms are larger than frictional terms which is of great importance for many fluid flows such as air and water. For the assumption of irrotational flows, the streamlines are a family of concentric circles. On top of that, the physical significance of the new solutions is shown by the fact that although the solution does not satisfy the no-slip conditions at the boundary, they are useful since they help to detect the response of atmospheric turbulence of the aircraft and the vortex free flow of incompressible fluids. In Moffatt,[30] the role of helicity in fluid dynamics, in particular, its role in depleting nonlinearity in the Navier–Stokes equations is discussed.

Kelbin *et al.*[31] derived and analyzed the full three-dimensional system of incompressible constant-density Euler and Navier–Stokes equations under the assumption of helical symmetry. In particular, they derived various new conservation laws admitted by the model, in primitive variables, and using the vorticity formulation. A general helically symmetric setting was used, where all three velocity components and the pressure are generally nonzero, and may depend on the time t, the cylindrical radius r, and the helical variable

$$\xi = az + b\varphi. \tag{1}$$

In a general helically symmetric setting, no restrictive assumptions are made concerning the form of the velocity components or the pressure. The consideration is based exclusively on the independence from the third spatial variable which changes along each helix r = const and ξ = const. Thus, the flow has two spatial dimensions and is called (2+1)-dimensional in space-time. Since the spatial dimensions are reduced to two, but all three components of the velocity vector are nonzero, helical flows are often referred to as "$2\frac{1}{2}$-dimensional." In turbulence research, a flow is denoted as a *two-component flow* if one of the velocity components vanishes.

Helical invariance of the Navier–Stokes equations is a consequence of its admitted Lie group of point symmetries, specifically, the invariance of the model with respect to rotations and translations about the z-axis. The helical invariance, thus, generalizes and includes the axial symmetry (achieved at $a = 1$, $b = 0$) and the z-translation symmetry (corresponding to $a = 0$, $b = 1$). In 2017, Dierkes and Oberlack extended the work of Kelbin *et al.*[31] by introducing a more general, time-dependent helical coordinate system, based on rotation and Galilei invariance of the Navier–Stokes model. The new approach used a time-dependent helical variable $\xi = z/\alpha(t) + b\varphi$, with b = const, and $\alpha(t) \neq 0$ is an arbitrary function of time t. This coordinate system describes helical flows with a time-dependent helical pitch; both Euler and Navier–Stokes equations admit a reduced invariant form with respect to this extended helical coordinate system.

The goal of the current contribution is to seek nontrivial, time-dependent exact solutions of the full helically invariant Navier–Stokes model. The study is motivated by the lack of such exact solutions, cf.Ref. 33, and, in particular, the development of specialized high-precision numerical codes, which require exact solutions for the code precision testing (see, e.g., Ref. 34).

The paper is organized as follows. In Sec. II, we present the general helically symmetric Navier–Stokes equations in the primitive variables and in the vorticity formulation. These formulas have been derived in Kelbin *et al.*[31] and generalize the helically invariant inviscid model discussed in Alekseenko *et al.*[35]

In Sec. III A, we consider the reduction of the helically invariant Navier–Stokes equations arising from the Galilei symmetry group admitted in terms of helical coordinates. A new nonlinear PDE (25) is derived describing such flows, and its particular exact solutions are constructed, giving rise to two families of time-dependent helically invariant incompressible viscous flows.

The second exact solution family is obtained in Sec. III B, where the vorticity formulation and Beltrami flow ansatz (collinearity of the velocity and vorticity) are used to construct global periodic helically invariant flows with radial dependence given in terms of confluent Heun functions.

The paper is concluded with discussion in Sec. IV. Computation details of the *v-equation* (25) and the periodic solutions (59) are provided in Appendices A and B, respectively.

II. HELICALLY INVARIANT NAVIER–STOKES EQUATIONS

In 2013, Kelbin *et al.*[31] introduced the helical coordinate system (r, η, ξ), which is given by

$$\xi = az + b\varphi, \quad \eta = a\varphi - bz/r^2, \tag{2}$$

where $a, b = \text{const}$, $a^2 + b^2 > 0$, and (r, φ, z) are the usual cylindrical coordinates.

On each cylinder $r = \text{const}$, the lines $\xi = \text{const}$ and $\eta = \text{const}$ correspond to two families of helices which are orthogonal to each other. By choosing the constants a, b, one obtains a specific helical frame. In the limiting case, if $a = 1$ and $b = 0$, the helical coordinates become cylindrical coordinates with $\eta = \varphi$ and $\xi = z$. Importantly, the curvilinear helical coordinates (r, η, ξ) do not form an orthogonal triple. Although the unit direction vectors of the coordinates r, ξ are orthogonal, it can be shown that there is no third coordinate that is orthogonal to both r and ξ and that can be consistently introduced in any open ball $B \in \mathbb{R}^3$. A locally orthogonal triple of unit vectors,

$$\boldsymbol{e}_r = \frac{\nabla r}{|\nabla r|}, \quad \boldsymbol{e}_\xi = \frac{\nabla \xi}{|\nabla \xi|}, \quad \boldsymbol{e}_{\perp\eta} = \frac{\nabla_\perp \eta}{|\nabla_\perp \eta|} = \boldsymbol{e}_\xi \times \boldsymbol{e}_r,$$

is defined at every point for the purpose of expansion of vector quantities in a natural basis (Fig. 1).

We define a *helically invariant* function as a function which is independent of η and has the form $F(t, r, \xi)$. We will assume that all physical variables are η-independent such that we obtain exact solutions for helically invariant flows. Throughout the paper, upper indices will refer to the corresponding components of vector fields (vorticity, velocity, etc.), and lower indices will denote partial derivatives. For example,

$$u^\eta_\xi \equiv \frac{\partial}{\partial \xi} u^\eta(t, r, \xi).$$

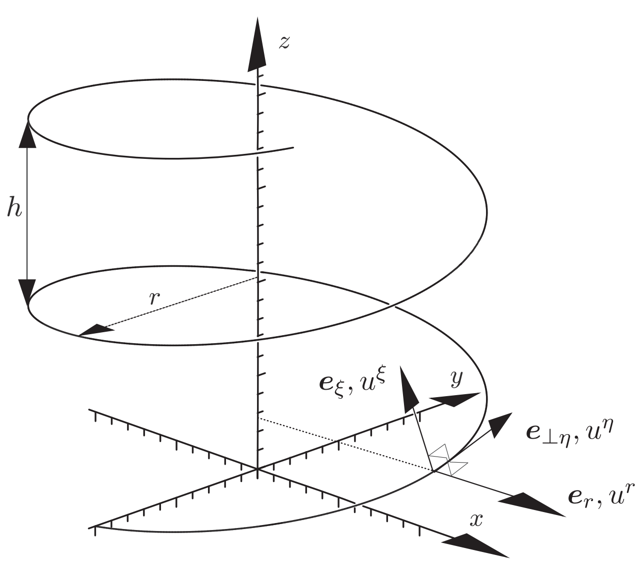

FIG. 1. An illustration of the helix $\xi = \text{const}$ for $a = 1$, $b = -h/2\pi$, where h is the z-step over one helical turn. Basis unit vectors in the helical coordinates.

We also assume summation in all repeated indices.

In the nabla-based notation in Cartesian coordinates, the Navier–Stokes equations of incompressible viscous fluid flows without external forces are given by

$$\nabla \cdot \boldsymbol{u} = 0, \tag{3a}$$

$$\boldsymbol{u}_t + (\boldsymbol{u} \cdot \nabla)\boldsymbol{u} + \nabla p - \nu \nabla^2 \boldsymbol{u} = 0, \tag{3b}$$

where the fluid velocity vector $\boldsymbol{u} = u^1\boldsymbol{e}_x + u^2\boldsymbol{e}_y + u^3\boldsymbol{e}_z$ and fluid pressure p, in which the density has already been absorbed, are functions of $\boldsymbol{x} = (x, y, z)$ and t. The viscosity coefficient $\nu = \text{const}$; the inviscid case $\nu = 0$ yields the Euler equations.

In order to rewrite Eq. (3) in a helically symmetric setting, one may write the velocity vector in the cylindrical and the helical basis,

$$\boldsymbol{u} = u^r\boldsymbol{e}_r + u^\varphi\boldsymbol{e}_\varphi + u^z\boldsymbol{e}_z = u^r\boldsymbol{e}_r + u^\eta\boldsymbol{e}_{\perp\eta} + u^\xi\boldsymbol{e}_\xi, \tag{4}$$

where u^r, u^φ, u^z are the velocity components in cylindrical coordinates. The helical velocity components are related to the cylindrical velocity components by

$$u^\eta = \boldsymbol{u} \cdot \boldsymbol{e}_{\perp\eta} = B\left(au^\varphi - \frac{b}{r}u^z\right), \quad u^\xi = \boldsymbol{u} \cdot \boldsymbol{e}_\xi = B\left(\frac{b}{r}u^\varphi + au^z\right), \tag{5}$$

and backward,

$$u^\varphi = B\left(au^\eta + \frac{b}{r}u^\xi\right), \qquad u^z = B\left(-\frac{b}{r}u^\eta + au^\xi\right), \tag{6}$$

where

$$B(r) = \frac{r}{\sqrt{a^2r^2 + b^2}}. \tag{7}$$

In what follows, for brevity, we will write $B(r) = B$ and $dB(r)/dr = B'$.

By transforming the PDEs to helical coordinates and assuming helical invariance $\partial/\partial\eta \equiv 0$ for all velocity components and the pressure, one obtains the continuity equation and the three components of the vector momentum equation, which represent the *helically invariant Navier–Stokes system in primitive variables*,

$$\frac{1}{r}u^r + u^r_r + \frac{1}{B}u^\xi_\xi = 0, \tag{8a}$$

$$u^r_t + u^r u^r_r + \frac{1}{B}u^\xi u^r_\xi - \frac{B^2}{r}\left(\frac{b}{r}u^\xi + au^\eta\right)^2 = -p_r + \nu\left[\frac{1}{r}(ru^r_r)_r + \frac{1}{B^2}u^r_{\xi\xi} - \frac{1}{r^2}u^r - \frac{2bB}{r^2}\left(au^\eta_\xi + \frac{b}{r}u^\xi_\xi\right)\right], \tag{8b}$$

$$u^\eta_t + u^r u^\eta_r + \frac{1}{B}u^\xi u^\eta_\xi + \frac{a^2B^2}{r}u^r u^\eta = \nu\left[\frac{1}{r}(ru^\eta_r)_r + \frac{1}{B^2}u^\eta_{\xi\xi} + \frac{a^2B^2(a^2B^2 - 2)}{r^2}u^\eta + \frac{2abB}{r^2}\left(u^r_\xi - \left(Bu^\xi\right)_r\right)\right], \tag{8c}$$

$$u^\xi_t + u^r u^\xi_r + \frac{1}{B} u^\xi u^\xi_\xi + \frac{2abB^2}{r^2} u^r u^\eta + \frac{b^2B^2}{r^3} u^r u^\xi = -\frac{1}{B} p_\xi$$
$$+ \nu\left[\frac{1}{r}(r u^\xi_r)_r + \frac{1}{B^2} u^\xi_{\xi\xi} + \frac{a^4B^4 - 1}{r^2} u^\xi\right.$$
$$\left. + \frac{2bB}{r}\left(\frac{b}{r^2} u^r_\xi + \left(\frac{aB}{r} u^\eta\right)_r\right)\right], \tag{8d}$$

where the velocity components u^r, u^η, u^ξ and the pressure p are functions of r, ξ and t, and the geometric factor B is given by (7). Due to the 2π-periodicity of the cylindrical polar angle φ, in order to be globally defined, every component of a helically invariant solution must be periodic in ξ with the period

$$\tau_\xi = 2\pi b. \tag{9}$$

The helically invariant reduction (8) of the Navier–Stokes equations has been extensively investigated in Kelbin *et al.*,[31] where various new conservation laws, including families of conservation laws, have been found for the viscous ($\nu \neq 0$) and the inviscid ($\nu = 0$) case. As an example, for the inviscid case, conservation laws of kinetic energy and z-projections of momentum and angular momentum have been found to hold, as well as new infinite families of generalized momenta/angular momenta conservation laws and the conservation of helicity. For the viscous case, a z-projection of momentum and an additional momentum-like quantity $(r/B)u^\eta$ are conserved.

The vorticity formulation of the Navier–Stokes equations (3) consists of the continuity equation, the definition of vorticity, and the vorticity dynamics equation obtained by taking the curl of the momentum equation (3b). It has the form

$$\nabla \cdot \boldsymbol{u} = 0, \tag{10a}$$

$$\boldsymbol{\omega} = \nabla \times \boldsymbol{u}, \tag{10b}$$

$$\boldsymbol{\omega}_t + \nabla \times (\boldsymbol{\omega} \times \boldsymbol{u}) - \nu\nabla^2 \boldsymbol{\omega} = 0, \tag{10c}$$

where it is worth noting that the latter have a reduced solution space, compared to (3) (see, e.g., Refs. 17 and 36). In the helical basis, the vorticity vector $\boldsymbol{\omega}$ is given by

$$\boldsymbol{\omega} = \omega^r \boldsymbol{e}_r + \omega^\eta \boldsymbol{e}_{\perp\eta} + \omega^\xi \boldsymbol{e}_\xi. \tag{11}$$

Under the assumption of helical invariance, the respective components of $\boldsymbol{\omega}$ are given by

$$\omega^r = -\frac{1}{B} u^\eta_\xi, \tag{12a}$$

$$\omega^\eta = \frac{1}{B} u^r_\xi - \frac{1}{r}\left(r u^\xi\right)_r - \frac{2abB^2}{r^2} u^\eta + \frac{a^2B^2}{r} u^\xi, \tag{12b}$$

$$\omega^\xi = u^\eta_r + \frac{a^2B^2}{r} u^\eta. \tag{12c}$$

At this point, it is worth noting that in three dimensions, the pseudo-vector $\boldsymbol{\omega}$ is itself a conserved quantity [for this type of partial solutions of the Navier–Stokes equations (3)], since all three components of the vorticity Eq. (10c) are, indeed, divergence expressions, with the components of $\boldsymbol{\omega}$ being the conserved densities. For the helically symmetric Navier–Stokes equations in vorticity formulation, multiple new vorticity-dependent conservation laws have been derived in the work of Kelbin *et al.*[31] These results have been extended in the work of Dierkes and Oberlack[32] to helically invariant flows with a time-dependent variable pitch.

III. EXACT SOLUTIONS TO THE HELICALLY INVARIANT NAVIER–STOKES EQUATIONS

In the current section, we present two different approaches to obtain exact solutions of the helically invariant Navier–Stokes equations. First, in Sec. III A, a Galilei-invariant reduction of the primitive Eq. (8) is considered. In Sec. III B, separated solutions corresponding to helically invariant Beltrami flows are constructed.

A. A reduction with respect to Galilei group in helical coordinates

The helically invariant Navier–Stokes equations (8) admit four independent point symmetry groups: translations in space ξ and time t, translation of the pressure p, and Galilean invariance in the ξ-direction. If the transformed quantities for each group G^i, $i = 1, 4$ are denoted by $\left(r^*, \xi^*, t^*, (u^r)^*, (u^\xi)^*, (u^\eta)^*, p^*\right) = G^i\left(r, \xi, t, u^r, u^\xi, u^\eta, p\right)$, one has

$$G^1 = \left(r, \xi + \varepsilon, t, u^r, u^\xi, u^\eta, p\right), \tag{13a}$$

$$G^2 = \left(r, \xi, t + \varepsilon, u^r, u^\xi, u^\eta, p\right), \tag{13b}$$

$$G^3 = \left(r, \xi, t, u^r, u^\xi, u^\eta, p + \varepsilon f(t)\right), \tag{13c}$$

$$G^4 = \left(r, \xi + \varepsilon t, t, u^r, u^\xi + \varepsilon B(r), u^\eta - \varepsilon \frac{b}{ar} B(r), p\right), \tag{13d}$$

where ε is the group parameter of the point symmetry groups. We note that no additional symmetries arise for two-component flows, where the velocity component in the invariant direction vanishes, $u^\eta \equiv 0$.

The infinitesimal generators corresponding to the symmetry groups (13) are given by

$$X_1 = \frac{\partial}{\partial t}, \tag{14a}$$

$$X_2 = \frac{\partial}{\partial \xi}, \tag{14b}$$

$$X_3 = f(t)\frac{\partial}{\partial p}, \tag{14c}$$

$$X_4 = t\frac{\partial}{\partial \xi} - \frac{b}{ar} B \frac{\partial}{\partial u^\eta} + B\frac{\partial}{\partial u^\xi}. \tag{14d}$$

For the Galilei symmetry G^4, X_4, we consider an invariant solution ansatz (see, e.g., Ref. 28). A solution $\boldsymbol{u} = \boldsymbol{\Theta}(r, t, \xi)$ with components $\boldsymbol{u} = \left(u^r, u^\xi, u^\eta, p\right)$ and $\boldsymbol{\Theta} = \left(\Theta^r, \Theta^\xi, \Theta^\eta, \Theta^p\right)$ is an invariant solution of the PDE system (8) with respect to the point symmetry (14d) if and only if $\boldsymbol{u} = \boldsymbol{\Theta}(r, t, \xi)$ satisfies

$$X_4(\boldsymbol{u} - \boldsymbol{\Theta}(r, \xi, t))|_{\boldsymbol{u}=\boldsymbol{\Theta}(r,\xi,t)} = 0. \tag{15}$$

This leads to the characteristic ODE system given by

$$\frac{du^r}{0} = -\frac{ar}{bB}du^\eta = \frac{du^\xi}{B} = \frac{d\xi}{t} = \frac{dr}{0} = \frac{dt}{0} = \frac{dp}{0}. \tag{16}$$

The zeros in the denominators of (16) denote that the corresponding variable in the numerator is constant. This denotation is frequently used when the method of characteristics is applied (see, e.g., Ref. 28) and may not be seen as an algebraic denotation. The invariants for the independent variables are given by

$$I_1 = r, \quad I_2 = t, \tag{17}$$

and for the dependent variables, (16) leads to a form, which is slightly generalized to

$$u^r = u^r(r,t), \tag{18a}$$

$$u^\xi = F^\xi(r,t)\xi + G^\xi(r,t), \tag{18b}$$

$$u^\eta = F^\eta(r,t)\xi + G^\eta(r,t), \tag{18c}$$

$$p = p(r,t), \tag{18d}$$

where $u^r(r, t)$, $F^\xi(r, t)$, $G^\xi(r, t)$, $F^\eta(r, t)$, $G^\eta(r, t)$, and $p(r, t)$ are to be determined. The substitution of (18) into the Navier–Stokes equations (8) leads to quadratic expressions in ξ, where all other unknown functions do not depend on ξ. Hence, all coefficients at independent expressions involving ξ must vanish. Consequently, as it is shown in Appendix A, which contains further details on the derivation of some subsequent equations, one obtains the restrictions,

$$F^\eta = -\frac{b}{ar}F^\xi \tag{19}$$

and

$$F^\xi = -\frac{B}{r}\left(ru^r\right)_r, \tag{20}$$

relating the unknown functions F^η, F^ξ, and u^r. This leads to rewriting the helically invariant Navier–Stokes equations (8) as a system of four ξ-independent PDEs for the unknowns u^r, G^ξ, G^η, and p, given by

$$u^r_t + u^r u^r_r - \frac{B^2}{r}\left(\frac{b}{r}G^\eta + aG^\xi\right)^2 + p_r - \nu\left[u^r_{rr} + \frac{1}{r}u^r_r - \frac{1}{r^2}u^r\right] = 0, \tag{21a}$$

$$ru^r_{rt} + u^r_t - u^r u^r_r - r\left(u^r_r\right)^2 + ru^r u^r_{rr} - \frac{2}{r}\left(u^r\right)^2 + \nu\left[-ru^r_{rrr} - 2u^r_{rr} - \frac{u^r}{r^2} + \frac{1}{r}u^r_r\right] = 0, \tag{21b}$$

$$G^\eta_t + u^r G^\eta_r + \frac{1}{B}G^\xi F^\eta + \frac{a^2B^2}{r}u^r G^\eta - \nu B\left[\frac{B''}{B^2}G^\eta + \frac{2B'}{B^2}G^\eta_r - \frac{2abB}{r^2}G^\xi_r - \left(\frac{2ab}{r^2}G^\xi + \frac{b^2 - a^2r^2}{r^3}G^\eta\right)B' - \frac{B}{r^3}\left(b^2 - a^2r^2\right)G^\eta_r + \frac{1}{B}G^\eta_{rr} + \frac{(b^2 - a^2r^2)B}{r^4}G^\eta\right] = 0, \tag{21c}$$

$$G^\xi_t + u^r G^\xi_r + \frac{1}{B}G^\xi F^\xi + \frac{2abB^2}{r^2}u^r G^\eta + \frac{b^2B^2}{r^3}u^r G^\xi - \nu B \times \left[\frac{B''}{B^2}G^\xi + \frac{2B'}{B^2}G^\xi_r + \frac{2abB}{r^2}G^\eta_r + \left(\frac{2ab}{r^2}G^\eta - \frac{b^2 - a^2r^2}{r^3}G^\xi\right)B' - \frac{B}{r^3}\left(b^2 - a^2r^2\right)G^\xi_r + \frac{1}{B}G^\xi_{rr} - \frac{2abB}{r^3}G^\eta\right] = 0. \tag{21d}$$

Importantly, the PDE (21b) for u^r decouples from the rest of the system of Eq. (21).

Substituting the ansatz expressions (18b) and (18c) into (6) and using (19), one finds that for the Galilei-invariant helical flows, the cylindrical polar angle velocity component u^φ reduces to

$$u^\varphi = B\left(aG^\eta + \frac{b}{r}G^\xi\right) \tag{22}$$

and is independent of F^ξ and F^η. A linear combination of (21c) and (21d), where (21c) is multiplied by aB and (21d) by bB/r, leads to a PDE for the u^φ-component, which is given by

$$u^\varphi_t + \frac{u^r u^\varphi}{r} + u^r u^\varphi_r - \nu\left(u^\varphi_{rr} + \frac{u^\varphi_r}{r} - \frac{u^\varphi}{r^2}\right) = 0. \tag{23}$$

Every solution of (21) yields a solution of the helically invariant Navier–Stokes equations (8)–(18). Solutions of the reduced system (21), in fact, are related to the solutions of a single PDE (21b). Indeed, for every solution u^r of (21b), one may find F^ξ and F^η from (20) and (19), respectively. In the next step, the solutions for F^ξ and F^η may be used to solve (21c) and (21d) for G^ξ and G^η. Interestingly, the PDEs (21c) and (21d) are linear PDEs for G^ξ and G^η with variable coefficients. Finally, one can obtain the pressure p from the PDE (21a).

The main Eq. (21b) can be brought into a particularly elegant form using the substitution

$$v(r,t) = r\,u^r(r,t), \tag{24}$$

leading to the PDE

$$v_{rt} + \left(\frac{vv_r}{r}\right)_r - 2\frac{v_r^2}{r} - \nu\left[v_{rrr} + \frac{v_r}{r^2} - \frac{v_{rr}}{r}\right] = 0, \tag{25}$$

satisfied by $v(r, t)$. In particular, the following statement holds: *every solution of the PDE (25) yields a solution of the helically invariant time-dependent Navier–Stokes equations (8).*

The *v-equation* (25) is a third-order nonlinear PDE which does not belong to any well-studied class of nonlinear PDEs, and for which, consequently, no exact solutions are known. The PDE (25) has a scaling symmetry and a translational symmetry in time, given by the infinitesimal generators,

$$Y_1 = r\frac{\partial}{\partial r} + 2t\frac{\partial}{\partial t}, \tag{26a}$$

$$Y_2 = \frac{\partial}{\partial t}. \tag{26b}$$

From (26), we generate the similarity variable

$$s = \frac{r}{\sqrt{4\nu(t + t_0)}} \tag{27}$$

to seek invariant solutions of the PDE (25) in the form $v = v(s)$, which yields the ODE

$$s^3 v'' + 2\,s\left(v'\right)^2 + s^2 v' - 2\,s v v'' + 2 v v' + v\left[2\,s^2 v''' - 2\,s v'' + 2 v'\right] = 0, \tag{28}$$

with prime denoting the derivative with respect to s. Two particular solution families of the ODE (28) can be readily constructed. The first solution family is obtained by demanding that both the linear and the nonlinear terms in (25) vanish separately, which leads to a consistent solution,

$$v(r,t) = A e^{-\frac{r^2}{4\nu(t+t_0)}}, \tag{29}$$

of the PDE (25), involving free constant parameters A and t_0. The second particular solution family is given by

$$v(r,t) = g(t) - \frac{r^2}{2(t+t_0)}, \tag{30}$$

where $g(t)$ is an arbitrary time-dependent function.

The next step in obtaining an explicit solution for the helically invariant flow is the solution of the (quite complex) linear PDEs (21c) and (21d) for the unknown functions G^ξ, G^η. A simple but explicit solution of the helically invariant Navier–Stokes system (8) can be immediately obtained if one assumes $G^\xi = G^\eta = 0$, which corresponds to a helically symmetric flow where the polar velocity component u^φ vanishes [cf. (22)], but all three helical velocity components u^r, u^η, and u^ξ remain nonzero. In this case, the solution (29) can be used to obtain the radial velocity component u^r using (24), the pressure using (21a), and the remaining velocity components (18b) and (18c) using (19) and (20). The full solution is given by

$$u^r = \frac{A}{r}\, e^{-\frac{r^2}{4\nu(t+t_0)}}, \quad u^\eta = -\frac{AbB\xi}{2\nu a r(t+t_0)}\, e^{-\frac{r^2}{4\nu(t+t_0)}}, \tag{31a}$$

$$u^\xi = \frac{AB\xi}{2\nu(t+t_0)}\, e^{-\frac{r^2}{4\nu(t+t_0)}}, \quad p = -\frac{A^2}{2r^2}\, e^{-\frac{r^2}{2\nu(t+t_0)}} + f(t), \tag{31b}$$

where $f(t)$ is an arbitrary function of time. In a similar manner, for the solution (30) of (25), one obtains the explicit exact solution,

$$u^r = \frac{g(t)}{r} - \frac{r}{2(t+t_0)}, \quad u^\eta = -\frac{bB\xi}{ar(t+t_0)}, \tag{32a}$$

$$u^\xi = \frac{B\xi}{t+t_0}, \quad p = -\frac{3}{8}\frac{r^2}{(t+t_0)^2} - \frac{g(t)^2}{2r^2} - g'(t)\,\ln r + h(t), \tag{32b}$$

involving an additional pressure gauge given by a function $h(t)$ which must be chosen such that the value of the pressure p remains positive. Unlike the first solution family (31), the second solution family (32) does not involve an arbitrary scaling parameter A.

We note again that both solutions (31) and (32) of the helically invariant Navier–Stokes equations (8) are neither periodic in ξ nor regular on the z-axis. These solutions should be understood as essentially local, i.e., defined in some helical annular sector, or in other words, a rectangle,

$$0 < r_1 \le r \le r_2, \quad 0 \le \xi_1 \le \xi \le \xi_2 < 2\pi b,$$

in the helical coordinates (r, ξ). This means that the solutions (31) and (32) are bounded in both directions, where r_1 is the lower and r_2 is the upper bound for the radial coordinate and ξ_1 and ξ_2 are the lower and upper bounds for the ξ-coordinate, respectively. Using the non-dimensionalization,

$$\hat r = r/b,\ \hat z = z/b,\ \hat\xi = \xi/b = a\hat z + \phi,\ \hat t = \nu t/b^2,$$

$$\hat u^r = u^r/u_0,\ \hat u^\eta = u^\eta/u_0,\ \hat u^\xi = u^\xi/u_0,\ \hat p = p/u_0^2,$$

$$\hat A = A/(bu_0),\ u_0 = \nu/b,\ \hat B = \hat r/\sqrt{a^2\hat r^2 + 1},$$

and the corresponding modifications of the arbitrary functions, the solutions (31) and (32) can be written, respectively, as

$$\hat u^r = \frac{\hat A}{\hat r}\, e^{-\frac{\hat r^2}{4(\hat t+\hat t_0)}}, \quad \hat u^\eta = -\frac{\hat A\hat B\hat\xi}{2a\hat r(\hat t+\hat t_0)}\, e^{-\frac{\hat r^2}{4(\hat t+\hat t_0)}}, \tag{33a}$$

$$\hat u^\xi = \frac{\hat A\hat B\hat\xi}{2(\hat t+\hat t_0)}\, e^{-\frac{\hat r^2}{4(\hat t+\hat t_0)}}, \quad \hat p = -\frac{\hat A^2}{2\hat r^2}\, e^{-\frac{\hat r^2}{2(\hat t+\hat t_0)}} + \hat f(\hat t), \tag{33b}$$

and

$$\hat u^r = \frac{\hat g(\hat t)}{r} - \frac{\hat r}{2(\hat t+\hat t_0)}, \qquad \hat u^\eta = -\frac{\hat B}{a\hat r\hat\xi(\hat t+\hat t_0)}, \tag{34a}$$

$$\hat u^\xi = \frac{\hat B\hat\xi}{\hat t+\hat t_0}, \quad \hat p = -\frac{3}{8}\frac{\hat r^2}{(\hat t+\hat t_0)^2} - \frac{\hat g(\hat t)^2}{2\hat r^2} - \hat g'(\hat t)\,\ln\hat r + \hat h(\hat t). \tag{34b}$$

For a flow with the velocity field $\boldsymbol{u}(t, \boldsymbol{x})$, the *instantaneous streamlines* are defined as parametric curves,

$$\frac{d}{d\gamma}\boldsymbol{x}(\gamma) = \boldsymbol{u}(t, \boldsymbol{x}(\gamma)), \quad \boldsymbol{x}(0) = \boldsymbol{x}_0, \tag{35}$$

where γ is a non-negative scalar parameter. For a generic time-dependent flow, instantaneous streamlines (35) change with time, and no fluid parcel has to follow any instantaneous streamline. On the other hand for equilibrium flows that are independent of time, as well as for special time-dependent flows, streamline curves can be fixed and, thus, followed by physical fluid parcels (Fig. 1).

For both of the above solutions, streamlines are curves in the plane ϕ = const. For the first solution family (33), the streamlines are not fixed but change in time since the time dependence of the velocity components is different; in particular, as $t \to \infty$, the streamlines tend to radial curves. For the second solution family (34), the streamlines are fixed if and only if $g(t) = 0$.

The dimensionless vorticity is defined as $\hat{\boldsymbol{\omega}} = b\boldsymbol{\omega}/u_0$, with components of $\boldsymbol{\omega}$ given by (12), and the dimensionless helicity density of the flow is computed as $\hat h = \hat{\boldsymbol{u}} \cdot \hat{\boldsymbol{\omega}}$.

For the first solution family (33), the velocity and vorticity magnitudes and the helicity density are given by

$$|\hat{\boldsymbol{u}}|^2 = \frac{\hat A^2 e^{-\frac{\hat r^2}{2(\hat t+\hat t_0)}}}{4a^2\hat r^2(\hat t+\hat t_0)^2}\left(4a^2(\hat t+\hat t_0)^2 + \hat r^2\hat\xi^2\right), \tag{36a}$$

$$|\hat{\boldsymbol{\omega}}|^2 = \frac{\hat A^2 e^{-\frac{\hat r^2}{2(\hat t+\hat t_0)}}}{16a^2\hat r^2(\hat t+\hat t_0)^4}\left(4(\hat t+\hat t_0)^2 + \hat r^4\hat\xi^2\right), \tag{36b}$$

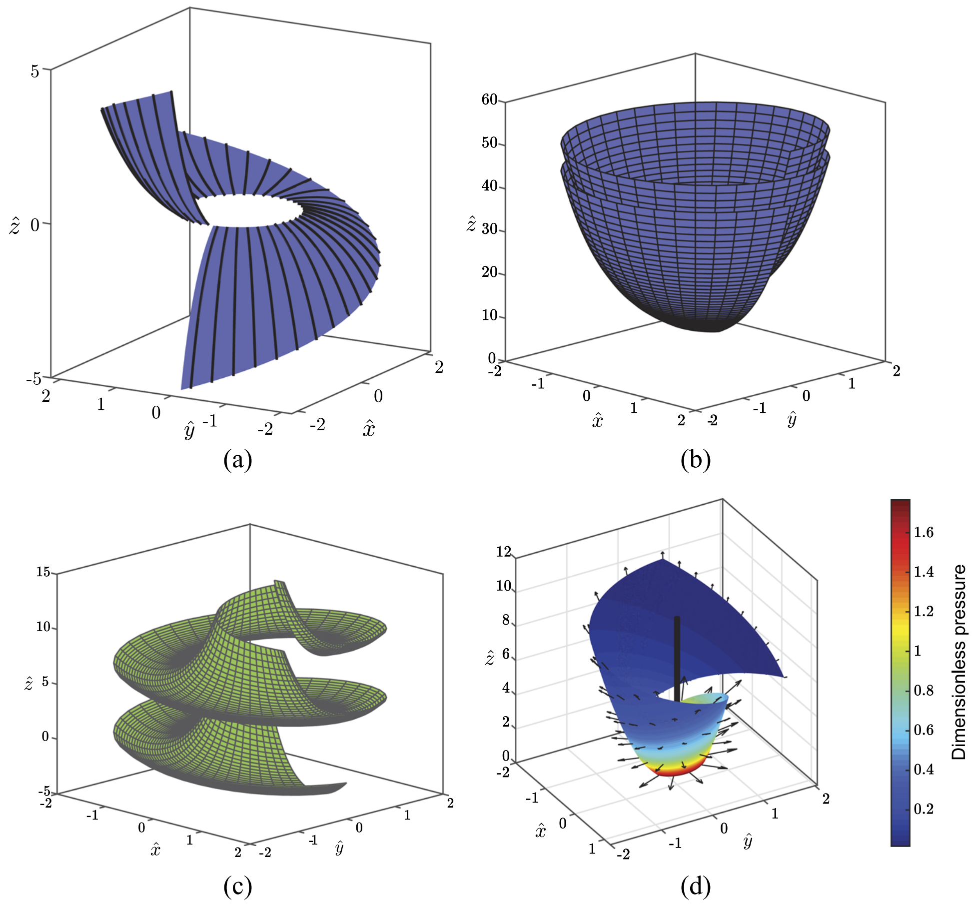

FIG. 2. Dimensionless flow parameters and the helical surface for the exact helically invariant solution (33) with $\hat{t} = 1$, $\hat{t}_0 = 0$, and $\hat{A} = \hat{f} = 1$. (a) The streamlines emanating from the circle $\hat{z} = 0, \hat{r} = 1$. (b) The velocity magnitude isosurface $|\hat{\boldsymbol{u}}| = 10$, plotted for $0 \le \phi \le 4\pi$, $\xi \ge 0$. (c) The vorticity magnitude isosurface $|\hat{\boldsymbol{\omega}}| = 2$, plotted for $0 \le \phi \le 4\pi$, $\xi \ge 0$. (d) The helical coordinate rectangle $\hat{\eta} = -6$, $0.5 \le \hat{r} \le 2$, and $0 \le \hat{\xi} \le 2\pi$ in the physical space, with velocity vectors and pressure $\hat{p}$ color map.

$$\hat{h} = \frac{\hat{A}^2 e^{-\frac{\hat{r}^2}{2(\hat{t}+\hat{t}_0)}}}{2a\hat{r}^2(\hat{t}+\hat{t}_0)}. \tag{36c}$$

Figure 2 shows streamlines, pressure profiles, the helical surface patch η = const, and examples of velocity and vorticity magnitude level surfaces $|\hat{\boldsymbol{u}}|$ = const and $|\hat{\boldsymbol{\omega}}|$ = const for the first solution family (33), for a sample set of dimensionless parameters.

For the second solution family (34), the velocity and vorticity magnitudes and the flow helicity density are given by

$$|\hat{\boldsymbol{u}}|^2 = \frac{a^2(2\hat{g}(\hat{t})(\hat{t}+\hat{t}_0) - \hat{r}^2)^2 + 4\hat{r}^2\hat{\xi}^2}{4a^2\hat{r}^2(\hat{t}+\hat{t}_0)^2}, \tag{37a}$$

$$|\hat{\boldsymbol{\omega}}| = \frac{1}{a\hat{r}(\hat{t}+\hat{t}_0)}, \tag{37b}$$

$$\hat{h} = \frac{\hat{g}}{a\hat{r}^2(\hat{t}+\hat{t}_0)} - \frac{1}{2a(\hat{t}+\hat{t}_0)^2}. \tag{37c}$$

In particular, in (37), for a fixed time t, the vorticity magnitude $|\hat{\boldsymbol{\omega}}|$ and the helicity density $\hat{h}$ are constant on circular cylinders r = const. We do not provide plots for this rather simple solution family because they are somewhat less physically appealing and can be obtained in a straightforward way.

B. The exact linearization of the Navier–Stokes equations; Beltrami-type solutions

The vector momentum equation in the Navier–Stokes model (3) is often written in the form

$$\boldsymbol{u}_t + (\mathit{curl}\,\boldsymbol{u}) \times \boldsymbol{u} + \nabla P - \nu\nabla^2\boldsymbol{u} = 0, \tag{38}$$

where the modified pressure is given by

$$P = p + \frac{1}{2}|\boldsymbol{u}|^2. \tag{39}$$

The essential nonlinearity is contained in the advection term (curl $\boldsymbol{u}$) $\times$ $\boldsymbol{u}$. The linearization idea of Beltrami consisted in setting it to zero, i.e., seeking exact solutions of the Navier–Stokes system that satisfy the *Beltrami flow* ansatz of vorticity and velocity collinearity,

$$\boldsymbol{\omega} \equiv \mathit{curl}\,\boldsymbol{u} = \vartheta\boldsymbol{u}, \tag{40}$$

where $\vartheta = \vartheta(\boldsymbol{x}, t)$ is an arbitrary scalar function. Beltrami flows have a deep physical meaning since it is known that every incompressible fluid flow is a superposition of Beltrami flows and every solution of the Navier–Stokes equations is a superposition of interacting Beltrami flows; cf. Ref. 37.

The seven scalar equations made up of the constant-density Navier–Stokes model (3) and the PDEs (40) make up an overdetermined linear system in terms of five unknown scalar functions given by $\boldsymbol{u}$, P, and ϑ. Even though overdetermined, these equations are known to have physically meaningful solutions (e.g., Refs. 17, 18, 26, and 38). It should be noted that due to the constraint (40), vortex stretching is inhibited in most cases, which is always the case for two-dimensional (2D) flows. Nevertheless, our newly found Beltrami-type exact solutions contain three nonzero velocity components and, hence, essentially differ from two-dimensional flows. Due to this discrepancy of the number of independent variables (the two helical coordinates r and ξ) and the three velocity components, the present flow and, hence, the solutions are still neither two- nor three-dimensional when the Beltramian restriction is employed. As before, the flow is placed between 2D and 3D, which we refer to as "$2\frac{1}{2}$-dimensional" and which is introduced in the first section of this article.

In the helically invariant setting, the subsequently presented linear equations (42) describing Beltrami flows follow from (8). They are given by seven PDEs for the unknowns $u^r(t, r, \xi)$, $u^\xi(t, r, \xi)$, $u^\eta(t, r, \xi)$, $P(t, r, \xi)$, and $\vartheta(t, r, \xi)$. The continuity equation reads

$$\frac{1}{r}u^r + (u^r)_r + \frac{1}{B}(u^\xi)_\xi = 0, \tag{41}$$

while the momentum equations reduce to the linear PDEs,

$$(u^r)_t = -P_r + \nu\left[\frac{1}{r}(r(u^r)_r)_r + \frac{1}{B^2}(u^r)_{\xi\xi} - \frac{1}{r^2}u^r - \frac{2bB}{r^2}\left(a(u^\eta)_\xi + \frac{b}{r}(u^\xi)_\xi\right)\right], \tag{42a}$$

$$(u^\eta)_t = \nu\left[\frac{1}{r}(r(u^\eta)_r)_r + \frac{1}{B^2}(u^\eta)_{\xi\xi} + \frac{a^2B^2(a^2B^2-2)}{r^2}u^\eta + \frac{2abB}{r^2}\left((u^r)_\xi - \left(Bu^\xi\right)_r\right)\right], \tag{42b}$$

$$(u^\xi)_t = -\frac{1}{B}P_\xi + \nu\left[\frac{1}{r}(r(u^\xi)_r)_r + \frac{1}{B^2}(u^\xi)_{\xi\xi} + \frac{a^4B^4-1}{r^2}u^\xi + \frac{2bB}{r}\left(\frac{b}{r^2}(u^r)_\xi + \left(\frac{aB}{r}u^\eta\right)_r\right)\right], \tag{42c}$$

and the three Beltrami conditions (40) together with the definition of the vorticity vector in helical coordinates in (12) are given by

$$\omega^r = -\frac{1}{B}(u^\eta)_\xi = \vartheta u^r, \tag{43a}$$

$$\omega^\eta = \frac{1}{B}(u^r)_\xi - \frac{1}{r}\left(ru^\xi\right)_r - \frac{2abB^2}{r^2}u^\eta + \frac{a^2B^2}{r}u^\xi = \vartheta u^\eta, \tag{43b}$$

$$\omega^\xi = (u^\eta)_r + \frac{a^2B^2}{r}u^\eta = \vartheta u^\xi. \tag{43c}$$

The linear homogeneous model (42) and (43) is autonomous in t and ξ and, thus, admits the separation of variable ansatz for all dependent variables,

$$q(t, r, \xi) = T(t)\,R(r)\,\Xi(\xi), \tag{44}$$

where q stands for each dependent variable: u^r, u^ξ, u^η, and P. Moreover, any linear combination of separated solutions (44) yields an exact solution of the linear homogeneous PDE system (42) and (43) and, thus, of the helically symmetric Navier–Stokes equations (8). All these solutions fulfill the Beltrami condition (40).

From the form of the momentum equation (42), consequently, an admissible form of the time dependence for the velocity components (and, hence, for the other unknowns, as it follows from the remaining PDEs) is given by exponential functions. In particular, for all velocity components, the time dependence is the same. Moreover, from the point of view of ξ-periodicity and the nature of differential relations, where spatial derivatives of the unknowns and the unknowns themselves are present in the equations, it is natural to assume the harmonic dependence of the unknowns on ξ: $\Xi(\xi) \sim \exp(i\lambda\xi)$, $\lambda = \text{const} \in \mathbb{R}$. For the linear homogeneous model, both the real and the imaginary part of each solution component yield solutions of the Beltrami model. (For simplicity, we will explicitly consider real functions.) From the form of Beltrami equations (40), consequently, the only admissible dependence of the Beltrami parameter ϑ is on the radial variable r. With the above assumptions, the general real form of the separated solutions is given by

$$u^r = e^{-\nu Q^2 t}(K_1\cos\lambda\xi + K_2\sin\lambda\xi)R_1(r), \tag{45a}$$

$$u^\xi = e^{-\nu Q^2 t}(K_3\cos\lambda\xi + K_4\sin\lambda\xi)R_2(r), \tag{45b}$$

$$u^\eta = e^{-\nu Q^2 t}(K_5\cos\lambda\xi + K_6\sin\lambda\xi)R_3(r), \tag{45c}$$

$$\vartheta = R_a(r), \tag{45d}$$

$$P = e^{-\nu Q^2 t}(K_7\cos\lambda\xi + K_8\sin\lambda\xi)R_p(r), \tag{45e}$$

where the parameters K_i, for $i = 1, \ldots, 8$, are constant. Their relation to the radial functions R_i, $i = 1, 2, 3$, R_a, and R_p in (45) are derived in Appendix B. The chosen form of the negative time exponent $-\nu Q^2 < 0$, $Q = \text{const} \in R$, is natural for the given parabolic problem (41) and (42). The exponentially decaying time-dependent term $e^{-\nu Q^2 t}$ makes the solutions (45) similar to the two-dimensional 2D Taylor's decaying vortices (e.g., Ref. 39).

Due to the periodicity of the helical variable ξ with its period given in Eq. (9), consequently, one must have

$$\lambda = \lambda_n = n/b, \quad n = 0, 1, 2, \ldots, \tag{46}$$

for natural numbers $n \in \mathbb{N}$, i.e., only discrete *modes* in the ξ-direction satisfy the periodicity conditions.

Furthermore, in Appendix B, it is shown that

$$\vartheta(r) = \text{const} = Q, \quad R_p(r) = 0.$$

Consequently, the modified pressure P is zero, which in turn leads to the final expression for the pressure,

$$p = p_0 - \frac{1}{2}|\boldsymbol{u}|^2, \quad p_0 = \text{const}, \tag{47}$$

and thus, the level surfaces of pressure and the velocity magnitude coincide. For physically meaningful solutions, the condition

$p_0 > \frac{1}{2}|\boldsymbol{u}|^2$ must hold, which ensures a non-negative pressure. It is further shown that the nonzero constants K_i in (45) are related by

$$\frac{K_2}{K_5} = -\frac{K_1}{K_6}, \quad \frac{K_3}{K_5} = \frac{K_4}{K_6}, \quad \frac{K_7}{K_8} = -\frac{K_4}{K_3}, \tag{48}$$

and $R_1(r)$ is a solution of a second-order ODE,

$$\frac{\mathrm{d}^2 R_1}{\mathrm{d}r^2} + \frac{B^2}{r}\left(\frac{3b^2}{r^2} + a^2\right)\frac{\mathrm{d}R_1}{\mathrm{d}r} - \left(\frac{\lambda^2}{B^2} + \frac{2a^2B^2 - 1}{r^2} - \vartheta^2 - \frac{2ab\vartheta B^2}{r^2}\right)R_1 = 0. \tag{49}$$

The remaining parameters $R_2(r)$ and $R_3(r)$ are related to $R_1(r)$ by

$$R_3 = -\frac{K_1}{K_6}\frac{\vartheta B}{\lambda}R_1, \quad R_2 = \frac{K_2}{K_3}\frac{B}{\lambda r}\left(R_1 + rR_1'\right). \tag{50}$$

ξ-dependent solutions are obtained for $\lambda \neq 0$, i.e., $n = 0$ in (46) such that the denominators in (50) are nonzero. Here and in the following, for functions depending on only one variable, we use the prime to denote the derivative with respect to that variable, e.g., $R_1' = \frac{\mathrm{d}R_1}{\mathrm{d}r}$. The general solution of the ODE (49) cannot be written in terms of elementary functions, but is related to the solution of the *confluent Heun ODE*,[40]

$$Y''(z) + \frac{\alpha z^2 + (\beta - \alpha + \gamma + 2)z + \beta + 1}{z(z-1)}Y'(z) + \frac{((\beta + \gamma + 2)\alpha + 2\delta)z - (\beta + 1)\alpha + (\gamma + 1)\beta + 2\sigma + \gamma}{2z(z-1)}Y(z) = 0, \tag{51}$$

involving five constant parameters α, β, γ, δ, and σ. Note that in contrast to Ref. 40, the fifth parameter in the confluent Heun ODE (51) is denoted by σ to avoid ambiguity with the third helical coordinate η defined in (2). While the original Heun ODE with an independent variable z has four singularities $z = 0$, $z = 1$, $z = a$, and $z = \infty$, the confluent Heun equation (51) is obtained from it by displacing the singularity $z = a$ to infinity, under an appropriate redefinition of the constant parameters (see, e.g., Ref. 41). Both the original Heun ODE and its confluent version are relatively well-studied (e.g., Refs. 41–44 and references therein). Existing literature includes asymptotic forms, recursion relations, series representations of Heun functions in terms of powers of z or hypergeometric functions, and so on. Heun functions are known to arise in various physical applications.[45] We also note that Heun functions can be efficiently numerically approximated.[46]

The solution of the ODE (49) is given by

$$R_1(r) = R_{1\,n}(r) = C_1 r^{n-1} H_{C^+} + C_2 r^{-n-1} H_{C^-}, \tag{52}$$

where C_1, C_2 are arbitrary constants, and

$$H_{C^+} = H_C\left(\alpha, \beta, \gamma, \delta, \sigma, -a^2r^2/b^2\right), \tag{53a}$$

$$H_{C^-} = H_C\left(\alpha, -\beta, \gamma, \delta, \sigma, -a^2r^2/b^2\right), \tag{53b}$$

are confluent Heun functions with parameters

$$\alpha = 0, \quad \beta = b\lambda_n = n, \quad \gamma = -2, \quad \delta = \frac{a^2n^2 - \vartheta^2b^2}{4a^2}, \quad \sigma = \frac{a^2(4 - n^2) + \vartheta b(2a + \vartheta b)}{4a^2}. \tag{54}$$

The remaining radial dependencies are found from (50) and are given by

$$R_2(r) = R_{2\,n}(r) = -\frac{K_1Bb}{K_4}\left(C_1r^{n-2}H_{C^+} - C_2r^{-n-2}H_{C^-}\right) + \frac{2K_1Ba^2}{K_4nb}\left(C_1r^nH_{C^+}' + C_2r^{-n}H_{C^-}'\right), \tag{55a}$$

$$R_3(r) = R_{3\,n}(r) = -\frac{K_1b\vartheta B}{K_6n}\left(C_1r^{n-1}H_{C^+} + C_2r^{-n-1}H_{C^-}\right). \tag{55b}$$

As mentioned before, all constants K_i including K_4 and K_6 are nonzero such that the radial functions R_2, R_3 are well-defined.

It is convenient to write the complete solution for the separated helical velocity components in terms of dimensionless variables,

$$\tilde{r} = \frac{ar}{b}, \quad \tilde{z} = \frac{az}{b}, \quad \tilde{\xi} = \tilde{z} + \varphi, \quad \tilde{t} = \nu\vartheta^2 t, \quad \gamma = \frac{b\vartheta}{a}, \quad \tilde{B}(\tilde{r}) = aB(\tilde{r}) = \frac{\tilde{r}}{\sqrt{\tilde{r}^2 + 1}}, \quad \tilde{\boldsymbol{u}} = \frac{b}{\nu}\boldsymbol{u}, \quad \tilde{p} = \frac{b^2}{\nu^2}p. \tag{56}$$

It is given by

$$\tilde{u}_n^r = e^{-\tilde{t}}\left(\tilde{C}_{1\,n}\tilde{r}^{n-1}H_{C^+} + \tilde{C}_{2\,n}\tilde{r}^{-n-1}H_{C^-}\right) \times \left(K_1\cos(n\tilde{\xi}) + K_2\sin(n\tilde{\xi})\right), \tag{57a}$$

$$\tilde{u}_n^\xi = e^{-\tilde{t}}\,\tilde{B}\left[\tilde{C}_{1\,n}\left(\tilde{r}^{n-2}H_{C^+} - \frac{2}{n}\tilde{r}^nH_{C^+}'\right) - \tilde{C}_{2\,n}\left(\tilde{r}^{-n-2}H_{C^-} + \frac{2}{n}\tilde{r}^{-n}H_{C^-}'\right)\right] \times \left(K_2\cos(n\tilde{\xi}) - K_1\sin(n\tilde{\xi})\right), \tag{57b}$$

$$\tilde{u}_n^\eta = e^{-\tilde{t}}\frac{\gamma\tilde{B}}{n}\left(\tilde{C}_{1\,n}\tilde{r}^{n-1}H_{C^+} + \tilde{C}_{2\,n}\tilde{r}^{-n-1}H_{C^-}\right) \times \left(K_2\cos(n\tilde{\xi}) - K_1\sin(n\tilde{\xi})\right), \tag{57c}$$

and the pressure $\tilde{p}$ is found from (47). In terms of dimensionless variables (56), the confluent Heun functions are given by

$$H_{C^\pm} = H_C\left(0, \pm n, -2, \frac{n^2 - \gamma^2}{4}, 1 + \frac{\gamma(\gamma + 2) - n^2}{4}, -\tilde{r}^2\right). \tag{58}$$

One may denote $K_1 = K\sin\psi$ and $K_2 = K\cos\psi$, where K, ψ is a different pair of arbitrary parameters [$K^2 = K_1 + K_2$, $\psi = \arctan(K_1/K_2)$]. Without loss of generality, we set $K = 1$. Then, (57) takes a simpler form,

$$\tilde{u}^r_n = e^{-\tilde{t}}\left(\tilde{C}_{1\,n}\,\tilde{r}^{n-1}H_{C^+} + \tilde{C}_{2\,n}\,\tilde{r}^{-n-1}H_{C^-}\right)\sin(n\tilde{\xi} + \psi_n), \tag{59a}$$

$$\tilde{u}^\xi_n = e^{-\tilde{t}}\,\tilde{B}\Big[\tilde{C}_{1\,n}\Big(\tilde{r}^{n-2}H_{C^+} - \frac{2}{n}\tilde{r}^n H'_{C^+}\Big) - \tilde{C}_{2\,n}\Big(\tilde{r}^{-n-2}H_{C^-} + \frac{2}{n}\tilde{r}^{-n}H'_{C^-}\Big)\Big]\cos(n\tilde{\xi} + \psi_n), \tag{59b}$$

$$\tilde{u}^\eta_n = e^{-\tilde{t}}\,\frac{\gamma\tilde{B}}{n}\left(\tilde{C}_{1\,n}\tilde{r}^{n-1}H_{C^+} + \tilde{C}_{2\,n}\tilde{r}^{-n-1}H_{C^-}\right)\cos(n\tilde{\xi} + \psi_n), \tag{59c}$$

$$\tilde{p}_n = p_{0\,n} - \frac{1}{2}\left(|\tilde{u}^r_n|^2 + |\tilde{u}^\xi_n|^2 + |\tilde{u}^\eta_n|^2\right). \tag{59d}$$

Depending on the choice of the constant parameters $n \in \mathbb{N}$ and $C_1, C_2, \gamma \in \mathbb{R}$, the separated space-time modes (59) may be bounded or unbounded functions, regular or singular at the origin. For example, for the choice $\tilde{C}_{2\,n} = 0$, $\gamma < 0$, and $n = 1, 2$, the radial parts of solution (59) components are bounded functions for all $\tilde{r}$ and are regular on the $\tilde{z}$-axis; for the same constants when $n \geq 3$, the Heun functions (58) diverge as $\tilde{r} \to \infty$. As an example, radial parts of the velocity component $\tilde{u}^r_n$ (59a) are shown in Fig. 3 for $n = 1, 2, 3$, $C_1 = 1$, $C_2 = 0$, and $\gamma = -3$.

While single-mode solutions present physical interest, since the Beltrami model (42) and (43) is linear and homogeneous, consequently, any linear combination of physical solutions (45),

$$\tilde{u}^r = \sum_n \tilde{u}^r_n, \quad \tilde{u}^\xi = \sum_n \tilde{u}^\xi_n, \quad \tilde{u}^\eta = \sum_n \tilde{u}^\eta_n, \quad \tilde{p} = \sum_n p_n \tag{60}$$

(involving arbitrary parameter families $\tilde{C}_{1\,n}$, $\tilde{C}_{2\,n}$, and ψ_n) yields a $\tilde{\xi}$-periodic physical exact solution of the helically invariant Navier–Stokes equations (8). We note that such solutions still have the same spatial period $\tau_{\tilde{\xi}}$ (9) in the $\tilde{\xi}$-direction.

It is important to remark that the time dependence both for modes (59) and for the general solution (60) is the same, i.e., all modes decay at the same rate. The following properties consequently hold for every solution:

1. The set of constant-pressure surfaces $\tilde{p}(\tilde{t}, \tilde{r}, \tilde{\xi}) = \text{const}$ [coinciding with level surfaces $|\boldsymbol{u}(\tilde{t}, \tilde{r}, \tilde{\xi})|^2 = \text{const}$ and $|\boldsymbol{\omega}(\tilde{t}, \tilde{r}, \tilde{\xi})|^2 = \text{const}$] are time-invariant, in the sense that the common time dependence factors out, and for the given value of $\tilde{p}$ (or $|\tilde{\boldsymbol{u}}|$, $|\tilde{\boldsymbol{\omega}}|$), the surfaces at different times $\tilde{t}$ are just different surfaces within the same set; no shape change occurs.
2. The streamlines (35) for the flow defined by an exact solution (60) are fixed and are followed by the particles. In particular, the velocity vector field never changes the direction, only changing its magnitude exponentially in time.

In Figs. 4(a) and 5(a), the cross section is periodic in $\tilde{\xi}$ with the period π, which is a half of the period $\tau_{\tilde{\xi}}$ (9) because the figures correspond to the isosurfaces of squared velocities. Note that these isosurfaces coincide with the isosurfaces of helicity density, since for all Beltrami flows, (40) holds, and the helicity density of such flows is given by $\tilde{h} = \vartheta|\tilde{\boldsymbol{u}}|^2$, with $\vartheta = \text{const} = Q$ for the solutions (59).

A sample set of upward-directed streamlines for the separated solution (59) with $n = 2$ is shown in Fig. 6. Both the solutions with $n = 1$ and $n = 2$ for the same set of other parameters include lines that are (on average) directed upward or downward. For some lines, the $\tilde{z}$-projection of the fluid velocity changes sign once or more per helical period.

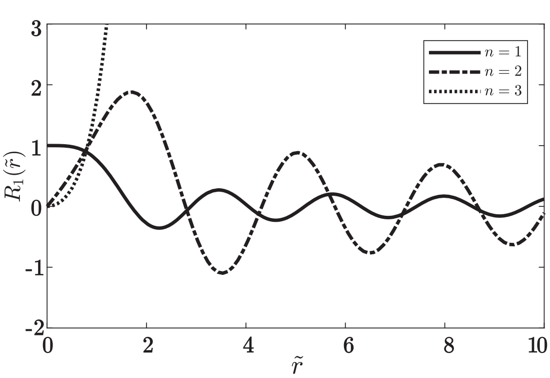

FIG. 3. An illustration of the radial part $R_{1\,n}(\tilde{r})$ (52) of the velocity component $\tilde{u}^r_n$ (59a) of the Beltrami solution (59) for $n = 1, 2, 3$, $\tilde{C}_{1\,n} = 1$, $\tilde{C}_{2\,n} = 0$, and $\gamma = -3$.

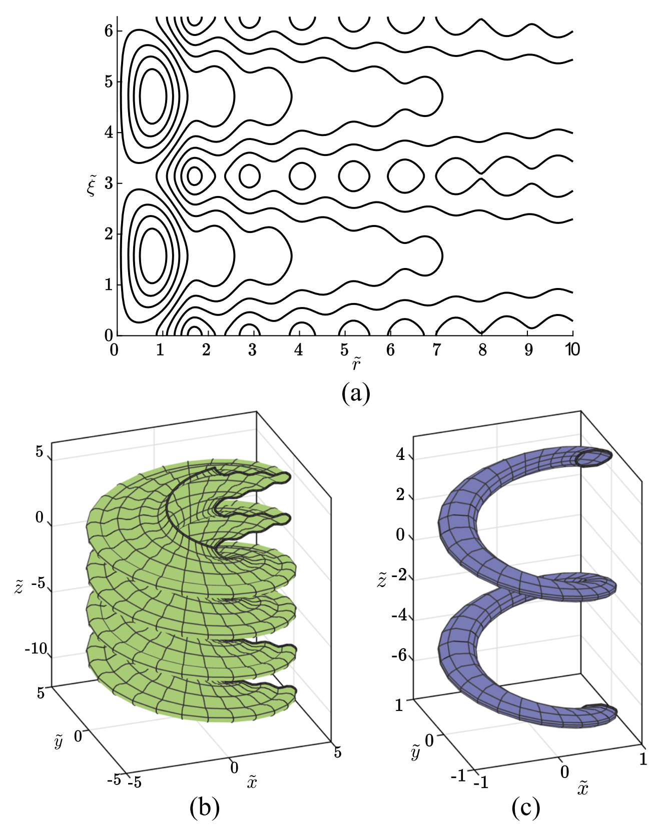

FIG. 4. Level surfaces $|\tilde{\boldsymbol{u}}|^2 = \text{const}$ (equivalently, $\tilde{p} = \text{const}$, $|\tilde{\boldsymbol{\omega}}|^2 = \text{const}$, or $\tilde{h} = \text{const}$) for the exact dimensionless Beltrami solution (59) for $n = 1$, $C_1 = 1$, $C_2 = 0$, and $\psi = -\pi/2$. (a) A cross section of level surface plot $|\tilde{\boldsymbol{u}}|^2 = \text{const}$, for one period $0 \leq \tilde{\xi} \leq 2\pi$. (b) A connected component of the level surface $|\tilde{\boldsymbol{u}}|^2 = 0.4$. (c) A connected component of the level surface $|\tilde{\boldsymbol{u}}|^2 = 2.6$.

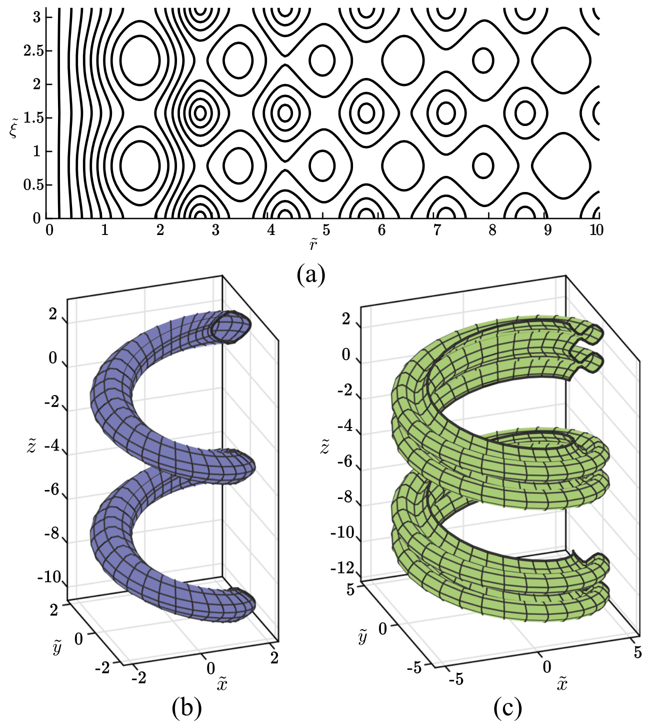

FIG. 5. Level surfaces $|\tilde{\boldsymbol{u}}|^2$ = const (equivalently, $\tilde{p}$ = const, $|\tilde{\boldsymbol{\omega}}|^2$ = const, or $\tilde{h}$ = const) for the exact dimensionless Beltrami solution (59) for $n = 2$, $C_1 = 1$, $C_2 = 0$, and $\psi = -\pi/2$. (a) A cross section of level surface plot $|\tilde{\boldsymbol{u}}|^2$ = const, for one period $0 \leq \tilde{\xi} \leq 2\pi$. (b) A connected component of the level surface $|\tilde{\boldsymbol{u}}|^2 = 3.54$. (c) A connected component of the level surface $|\tilde{\boldsymbol{u}}|^2 = 0.97$.

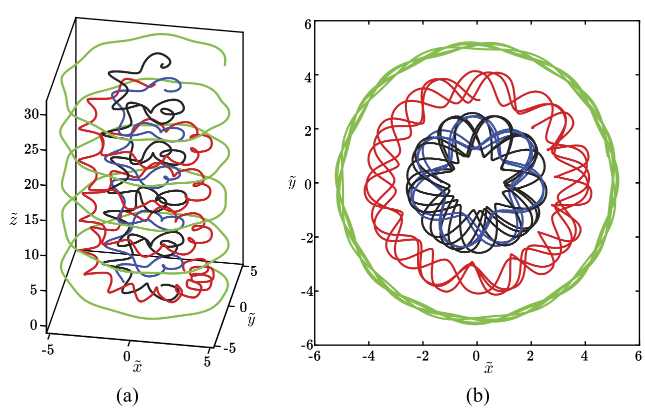

FIG. 6. Four sample streamlines for the exact dimensionless Beltrami solution (59) for $n = 2$, $C_1 = 1$, and $C_2 = 0$, emanating from various points in the plane $z = 1$. (a) Perspective view. (b) Top view.

IV. SUMMARY AND CONCLUSIONS

In the present contribution, we provide two types of exact solutions to the helically invariant system of Navier–Stokes equations. The first type arises from the invariant solution ansatz with respect to the Galilei group (13d) admitted by the helically invariant Navier–Stokes equations (8). We derive a new nonlinear PDE of third-order (25), for which we present two particular solutions, given by (29) and (30). From that, complete solutions to the Navier–Stokes system are derived and given by (31) and (32). It remains an open problem to derive further physically relevant particular solutions, as well as the general solution, of the v-equation (25). We verified that the v-equation does not admit nonclassical symmetries; hence, the nonclassical method (e.g., Ref. 28) and the equivalent "direct method" of Clarkson and Kruskal[47] cannot be used to construct additional exact solutions.

The second type of solutions for the helically invariant system of Navier–Stokes equations (8) is based on an exact linearization of the Navier–Stokes equations, where we seek solutions that satisfy the Beltrami condition (40). We note that for such flows, the most important mechanism in turbulence, the vortex stretching is not active since the velocity and the vorticity vectors are parallel. Nevertheless, in order to seek exact solutions, the Beltrami assumption is extremely helpful, as the PDE system (8) becomes linear. A family of separated solutions of this system is described by an exponential decay in time, ξ-periodic ansatz (45), leading to a linear system of ODEs [(B13) in Appendix B]. Exact solutions (59) were found in the case of constant Beltrami parameter ϑ. These solutions involve confluent Heun functions. While all such separated solutions are ξ-periodic, the radial dependence may be regular or singular on the z-axis, and the solutions may grow or decay as $r \to \infty$. However, all solutions (59) are regular in annular domains $0 < r_1 \leq r \leq r_2$. We also note that though the solutions (59) are time-dependent, all streamlines and level surfaces of helicity density, velocity, and vorticity magnitude are time-invariant (see Figs. 4–6).

All the newly derived exact solution families (31), (32), and (59) can be applied as benchmark tests for the development of helically invariant numerical codes. In particular, one application is the simulation of a flow between two coaxial cylinders extended by the axial motion of the inner cylinder.[48] The authors conducted simulations for different ratios of the radii and observed helically shaped turbulent patches. These flows are referred to as annular or sliding Couette flows. For such geometries, due to the presence of the inner cylinder, the centerline axis $r = 0$ is excluded, i.e., the radial coordinate is bounded by $0 < R_1 \leq r \leq R_2$ and the singular behavior vanishes. The exact solutions can be used as Dirichlet boundary conditions, which is the simplest case. In particular, it is possible to set

$$\boldsymbol{u}_{D,\mathrm{i}} = \boldsymbol{u}_{ex}(r = R_1, \xi) \tag{61}$$

at the wall of the inner cylinder and

$$\boldsymbol{u}_{D,\mathrm{o}} = \boldsymbol{u}_{ex}(r = R_2, \xi) \tag{62}$$

as the no-slip condition at the wall of the outer cylinder. Here, $\boldsymbol{u}_{ex}$ denotes the helical velocity vector of the exact solutions. Similarly, Dirichlet conditions can be assumed in the ξ-direction for the solutions (31) and (32) and periodic boundary conditions in this direction for the Beltrami solution (59). Besides the possibility to formulate boundary conditions, the solutions may be used to determine the errors and convergence rates of a numerical discretization of the helically invariant Navier–Stokes equations (8). Especially, the solution families (31) and (32) offer a great possibility of generating numerical tests quickly due to their simplicity.

The exact solutions derived in this paper exhibit different behaviors when the viscosity ν tends to zero. Indeed, in the limit $\nu \to 0^+$, for the solution (31), note that a reduction in length scales takes place; solutions (32) are independent of the viscosity; for solutions (59), time scales grow in the limit $\nu \to 0^+$, whereas length scales are not affected, as seen from formulas (56).

General local conservation laws of helically invariant Navier–Stokes equations, including those derived in Kelbin *et al.*,[31] hold for all solutions of the model. Additional conservation laws holding for restricted classes of solutions described by additional relations, such as the Beltrami condition (40), can theoretically arise. Such additional conservation laws can be found, for example, through the use of the direct (multiplier) method (see, e.g., Ref. 28) applied to the extended PDE system given by the original model equations and the additional relations. A detailed study of this possibility for fluid dynamics equations is a possible direction of future research.

Both types of exact time-dependent solutions of the Navier–Stokes equations derived in the current work are given by explicit closed-form expressions, suitable for further analysis and algebraic manipulation. For example, one can study the dynamics of points where the maximum of vorticity or its specific component(s) is achieved, referred to as the *vortex core* (e.g., Refs. 49 and 50) as well as their other local and global characteristics. In particular, for the exact solution (33), the dimensionless vorticity component in the invariant direction is given by

$$\hat{\omega}^{\eta} = \frac{\hat{A}\hat{B}\hat{r}\hat{\xi}}{4\left(\hat{t}+\hat{t}_0\right)^2}\, e^{-\frac{\hat{r}^2}{4(\hat{t}+\hat{t}_0)}}. \tag{63}$$

If the vortex core is defined as the maximal value of $|\omega^{\eta}|$ as a function of the cylindrical radius $\hat{r}$, one readily finds that the radial position of the vortex core is described by an increasing function,

$$\hat{r}^{\eta}_{max}(t) = \frac{1}{2a}\sqrt{4a^2\left(\hat{t}+\hat{t}_0\right) + 2\left(\sqrt{4a^4\left(\hat{t}+\hat{t}_0\right)^2 + 12a^2\left(\hat{t}+\hat{t}_0\right)+1} - 1\right)}. \tag{64}$$

Another possible direction of future research is to study the confluent Heun-type solutions (59) in more detail. Further physical solutions can possibly be found through equivalence transformations, other parameter choices, and linear combinations of various modes that may describe specific situations of interest.

ACKNOWLEDGMENTS

The authors are grateful to the Germany Research Foundation (DFG) under Grant No. OB 96/41-1 for financial support and the NSERC of Canada under Grant No. RGPIN-2014-05733 for research support.

APPENDIX A: DETAILS OF THE DERIVATION OF THE v-EQUATION (25)

The substitution of the ansatz (18) into the Navier–Stokes equations (8) yields

$$\frac{1}{r}\left(ru^r\right)_r + \frac{1}{B}F^{\xi} = 0, \tag{A1a}$$

$$\begin{aligned} &-\frac{B^2}{r}\left(\frac{b}{r}F^{\xi}+aF^{\eta}\right)^2\xi^2 - \frac{2B^2}{r}\left(\frac{b}{r}F^{\xi}+aF^{\eta}\right)\left(\frac{b}{r}G^{\eta}+aG^{\xi}\right)\xi \\ &+ u^r_t + u^r u^r_r - \frac{B^2}{r}\left(\frac{b}{r}G^{\eta}+aG^{\xi}\right)^2 \\ &+ p_r - \nu\left[u^r_{rr} + \frac{1}{r}u^r_r - \frac{1}{r^2}\left(u^r + \frac{2Bb^2}{r}F^{\xi} + 2abBF^{\eta}\right)\right] = 0, \end{aligned} \tag{A1b}$$

$$\begin{aligned} &\left[F^{\eta}_t + u^r F^{\eta}_r + \frac{F^{\xi}F^{\eta}}{B} + \frac{u^r F^{\eta} a^2 B^2}{r} - \nu B\left(\frac{F^{\eta}B''}{B^2} - \left(\frac{2ab}{r^2}F^{\xi} + \frac{\frac{b^2}{r^2}-a^2}{r}F^{\eta}\right)B' + \frac{2B'}{B^2}F^{\eta}_r - \frac{2abB}{r^2}F^{\xi}_r - \frac{B}{r}\left(\frac{b^2}{r^2}-a^2\right)F^{\eta}_r\right.\right. \\ &\left.\left. + \frac{1}{B}F^{\eta}_{rr} + \frac{B}{r^2}\left(\frac{b^2}{r^2}-a^2\right)F^{\eta}\right)\right]\xi + G^{\eta}_t + u^r G^{\eta}_r + \frac{G^{\xi}F^{\eta}}{B} + \frac{a^2B^2}{r}u^r G^{\eta} - \nu B\left[\frac{B''}{B^2}G^{\eta} - \left(\frac{2ab}{r^2}G^{\xi} + \frac{\frac{b^2}{r^2}-a^2}{r}G^{\eta}\right)B'\right. \\ &\left. + \frac{2B'}{B^2}G^{\eta}_r - \frac{2abB}{r^2}G^{\xi}_r - \frac{B}{r}\left(\frac{b^2}{r^2}-a^2\right)G^{\eta}_r + \frac{1}{B}G^{\eta}_{rr} + \frac{B}{r^2}\left(\frac{b^2}{r^2}-a^2\right)G^{\eta}\right] = 0, \end{aligned} \tag{A1c}$$

$$\begin{aligned} &\left[F^{\xi}_t + u^r F^{\xi}_r + \frac{1}{B}\left(F^{\xi}\right)^2 + \frac{2abB^2}{r^2}u^r F^{\eta} + \frac{b^2B^2}{r^3}F^{\xi}u^r - \nu B\left(\frac{B''}{B^2}F^{\xi} + \left(\frac{2ab}{r^2}F^{\eta} - \frac{\frac{b^2}{r^2}-a^2}{r}F^{\xi}\right)B' + \frac{2B'}{B^2}F^{\xi}_r + \frac{2abB}{r^2}F^{\eta}_r\right.\right. \\ &\left.\left. - \frac{B}{r}\left(\frac{b^2}{r^2}-a^2\right)F^{\xi}_r + \frac{1}{B}F^{\xi}_{rr} - \frac{2abB}{r^3}F^{\eta}\right)\right]\xi + G^{\xi}_t + u^r G^{\xi}_r + \frac{1}{B}G^{\xi}F^{\xi} + \frac{2abB^2}{r^2}u^r G^{\eta} + \frac{b^2B^2}{r^3}u^r G^{\xi} - \nu B \\ &\times\left[\frac{B''}{B^2}G^{\xi} + \left(\frac{2ab}{r^2}G^{\eta} - \frac{\frac{b^2}{r^2}-a^2}{r}G^{\xi}\right)B' + \frac{2B'}{B^2}G^{\xi}_r + \frac{2abB}{r^2}G^{\eta}_r - \frac{B}{r}\left(\frac{b^2}{r^2}-a^2\right)G^{\xi}_r + \frac{1}{B}G^{\xi}_{rr} - \frac{2abB}{r^3}G^{\eta}\right] = 0, \end{aligned} \tag{A1d}$$

where (A1a) is the continuity equation, (A1b) is the r-momentum equation, (A1c) is the η-momentum equation, and (A1d) is the ξ-momentum equation. In (A1), the coefficients of the powers ξ^2, ξ^1, and ξ^0 must vanish independently. The condition of a vanishing coefficient of the ξ^2-term of (A1b) leads to the relation (19),

$$F^\eta = -\frac{b}{ar}F^\xi.$$

Furthermore, the determining equations which arise from vanishing coefficients of the first-order terms $[O(\xi)]$ of the ξ-momentum and η-momentum are equivalent. Using the vanishing coefficient of the $O(\xi^0)$-terms of the continuity equation, we obtain condition (20), given by

$$F^\xi = -\frac{B}{r}(ru^r)_{,r},$$

and relating the unknown functions F^ξ and u^r. By substitution of this relation into the remaining helically invariant Navier–Stokes equations (8), one obtains a set of four determining PDEs for the unknowns u^r, G^ξ, G^η, and p, which is given by (21). Its second PDE is a decoupled equation for u^r, from which the v-equation (25) follows after the substitution (24).

APPENDIX B: DERIVATION OF THE PARAMETERS IN THE BELTRAMI FLOW ANSATZ (45)

The derivation of the parameters $K_1 - K_8$, $R_1 - R_3$, and R_p in (45) proceeds as follows: Employing the solution (45) into (43a) yields

$$\frac{e^{-\nu Q^2 t}}{B}(K_5\lambda\sin(\lambda\xi) - K_6\cos(\lambda\xi))R_3 = \vartheta(r)e^{-\nu Q^2 t}(K_1\cos(\lambda\xi) + K_2\sin(\lambda\xi))R_1, \tag{B1}$$

which may be simplified to

$$\left(\frac{K_5\lambda}{B}R_3 - K_2\vartheta R_1\right)\sin(\lambda\xi) - \left(\frac{K_6\lambda}{B}R_3 + K_1\vartheta R_1\right)\cos(\lambda\xi) = 0. \tag{B2}$$

For vanishing coefficients of (B2), we obtain

$$K_2 = \frac{K_5\lambda}{\vartheta B}\frac{R_3}{R_1}, \qquad K_1 = -\frac{K_6\lambda}{\vartheta B}\frac{R_3}{R_1}, \tag{B3}$$

which leads to

$$\frac{K_2}{K_5} = -\frac{K_1}{K_6}. \tag{B4}$$

Employing (45) into (43c), we obtain

$$\left(K_6\left(R_3' + \frac{a^2B^2}{r}R_3\right) - K_4\vartheta R_2\right)\sin(\lambda\xi) + \left(K_5\left(R_3' + \frac{a^2B^2}{r}R_3\right) - K_3\vartheta R_2\right)\cos(\lambda\xi) = 0. \tag{B5}$$

As before, vanishing coefficients yield

$$K_3 = \frac{K_5}{\vartheta R_2}\left(R_3' + \frac{a^2B^2}{r}R_3\right), \qquad K_4 = \frac{K_6}{\vartheta R_2}\left(R_3' + \frac{a^2B^2}{r}R_3\right), \tag{B6}$$

where

$$\frac{K_3}{K_5} = -\frac{K_4}{K_6}. \tag{B7}$$

Finally, employing (45) into (43b) leads to

$$\left(-\frac{K_1\lambda}{B}R_1 - \frac{K_4}{r}(rR_2)' - \frac{2K_6abB^2}{r^2}R_3 + \frac{K_4a^2B^2}{r}R_2 - K_6\vartheta R_3\right)\sin(\lambda\xi) + \left(-\frac{K_2\lambda}{B}R_1 - \frac{K_3}{r}(rR_2)' - \frac{2K_5abB^2}{r^2}R_3 + \frac{K_3a^2B^2}{r}R_2 - K_5\vartheta R_3\right) \times \cos(\lambda\xi) = 0. \tag{B8}$$

For vanishing coefficients of (B8), we obtain

$$K_5 = \frac{r^2}{(2abB^2 + \vartheta r^2)R_3}\left(-\frac{K_2\lambda}{B}R_1 - \frac{K_3}{r}(rR_2)' + \frac{K_3a^2B^2}{r}R_2\right), \tag{B9a}$$

$$K_6 = \frac{r^2}{(2abB^2 + \vartheta r^2)R_3}\left(-\frac{K_1\lambda}{B}R_1 - \frac{K_4}{r}(rR_2)' + \frac{K_4a^2B^2}{r}R_2\right). \tag{B9b}$$

Employing (45) into the continuity equation (41) leads to

$$\left(K_2R_1 + K_2rR_1' - K_3\lambda\frac{r}{B}R_2\right)\sin(\lambda\xi) + \left(K_1R_1 + K_1rR_1' - K_4\lambda\frac{r}{B}R_2\right)\cos(\lambda\xi) = 0. \tag{B10}$$

The coefficients yield

$$K_1 = -K_4\lambda\frac{r}{B}\frac{R_2}{R_1 + rR_1'}, \qquad K_2 = K_3\lambda\frac{r}{B}\frac{R_2}{R_1 + rR_1'}, \tag{B11}$$

which leads to

$$\frac{K_1}{K_4} = -\frac{K_2}{K_3}. \tag{B12}$$

The condition (B12) is a combination of (B4) and (B7). We now consider the system of linear ODE's, stemming from (B3), (B6), (B9b), and (B11) with nonlinear coefficients, given by

$$R_1 = -\frac{K_6}{K_1}\frac{\lambda}{\vartheta B}R_3, \tag{B13a}$$

$$R_2 = \frac{K_6}{\vartheta K_4}\left(R_3' + \frac{a^2B^2}{r}R_3\right), \tag{B13b}$$

$$R_3 = \frac{r^2}{K_6(2abB^2 + \vartheta r^2)}\left(-\frac{K_1\lambda}{B}R_1 - \frac{K_4}{r}(rR_2)' + \frac{K_4a^2B^2}{r}R_2\right), \tag{B13c}$$

$$R_2 = \frac{K_2}{K_3}\frac{B}{\lambda r}(R_1 + rR_1'), \tag{B13d}$$

which is a system for the unknowns R_1, R_2, R_3, and ϑ. The constraints for the parameters $K_1, \ldots, K_6$ are given by (B4) and (B7). Employing (B13a) and (B13d) into (B13b) and using the constraints (B4) and (B7) leads to $\vartheta' = 0$ and, hence, $\vartheta = const.$ The second-order ODE (49) may be derived by employing (B13a), (B13d), (B4), and (B7) into (B13c). As before, for the Beltrami equation (40), we employ the ansatz (45) into the momentum equations (42). From the momentum equation in the radial direction (42a), we obtain one additional constraint for the parameters, which is given by

$$\frac{K_7}{K_8} = -\frac{K_4}{K_3}. \tag{B14}$$

The solution of the ODE (49) is related to that of the confluent Heun ODE[40] with parameters (54), in which a and b are the helix pitch parameters [cf. (2)], $n \in \mathbb{N}$ is the ξ-mode number, and $\vartheta = \text{const}$ is the Beltrami parameter in (40). Here, we use the notation of the MAPLE-Software[51] package for the Confluent Heun function.

Specifically, the general solution of the ODE (49) is given by (52). From Eq. (B13), we obtain the exact solutions (55) for $R_2(r)$ and $R_3(r)$. A condition for the Beltrami parameter ϑ can be found by substitution of (45) and the derived solutions for $R_1(r)$, $R_2(r)$, and $R_3(r)$ into the η-projection of momentum (42b) and results in

$$\vartheta = Q. \tag{B15}$$

Furthermore, employing (45) and $R_1(r)$, $R_2(r)$, and $R_3(r)$ into the ξ-projection of momentum (42c) leads to the following equation for $R_p(r)$, given by

$$K_8 \lambda r \left(a^2 r^2 + b^2\right)^3 R_p(r) = 0, \tag{B16}$$

which has the solution $R_p(r) = 0$. Hence, from (45e), consequently, the modified pressure P is zero, which in turn leads to the final solution for the pressure, given by (47). Finally, (B14) may be written as

$$K_7 = -K_8 \frac{K_4}{K_3}. \tag{B17}$$

Assuming that $K_8 = 0$, it follows from (B17) that $K_7 = 0$. This also leads to the result that $P = 0$, which can be seen from (45e).

DATA AVAILABILITY

Data sharing is not applicable to this article as no new data were created or analyzed in this study.

REFERENCES

[1] L. J. Vermeer, J. N. Sørensen, and A. Crespo, "Wind turbine wake aerodynamics," Prog. Aerosp. Sci. **39**, 467–510 (2003).

[2] A. Mitchell, S. Morton, and J. Forsythe, "Wind turbine wake aerodynamics," Report No. ADA425027, Air Force Academy Colorado Springs, Department of Aeronautics, 1997.

[3] O. I. Bogoyavlenskij, "Helically symmetric astrophysical jets," Phys. Rev. E **62**, 8616–8627 (2000).

[4] D. D. Schnack, E. J. Caramana, and R. A. Nebel, "Three-dimensional magnetohydrodynamic studies of the reversed-field pinch," Phys. Fluids **28**, 321–333 (1985).

[5] J. L. Johnson, C. R. Oberman, R. M. Kulsrud, and E. A. Frieman, "Some stable hydromagnetic equilibria," Phys. Fluids **1**, 281–296 (1958).

[6] T. Sarpkaya, "On stationary and travelling vortex breakdowns," J. Fluid Mech. **45**, 545–559 (1971).

[7] S. L. Bragg and W. R. Hawthorne, "Some exact solutions of the flow through annular cascade actuator discs," J. Aeronaut. Sci. **17**, 243–249 (1950).

[8] H. Grad and H. Rubin, "Hydromagnetic equilibria and force-free fields," J. Nucl. Energy **7**, 284–285 (1958).

[9] V. D. Shafranov, "Propagation of an electromagnetic field in a medium with spatial dispersion," Sov. Phys. JETP **7**, 1019–1029 (1958).

[10] O. I. Bogoyavlenskij, "Exact helically symmetric plasma equilibria," Lett. Math. Phys. **51**, 235–247 (2000).

[11] A. F. Cheviakov and O. I. Bogoyavlenskij, "Exact anisotropic MHD equilibria," J. Phys. A: Math. Gen. **37**, 7593 (2004).

[12] C. Y. Wang, "On the low-Reynolds-number flow in a helical pipe," J. Fluid Mech. **108**, 185–194 (1981).

[13] M. Germano, "On the effect of torsion on a helical pipe flow," J. Fluid Mech. **125**, 1–8 (1982).

[14] M. Germano, "The Dean equations extended to a helical pipe flow," J. Fluid Mech. **203**, 289–305 (1989).

[15] E. R. Tuttle, "Laminar flow in twisted pipes," J. Fluid Mech. **219**, 545–570 (1990).

[16] L. Zabielski and A. J. Mestel, "Steady flow in a helically symmetric pipe," J. Fluid Mech. **370**, 297–320 (1998).

[17] S. V. Ershkov, R. V. Shamin, and A. R. Giniyatullin, "On a new type of non-stationary helical flows for incompressible 3D Navier-Stokes equations," J. King Saud Univ., Sci. **32**(1), 459–467 (2020).

[18] S. V. Ershkov, "Non-stationary helical flows for incompressible 3D Navier–Stokes equations," Appl. Math. Comput. **274**, 611–614 (2016).

[19] I. Delbende, M. Rossi, and O. Daube, "DNS of flows with helical symmetry," Theor. Comput. Fluid Dyn. **26**, 141–160 (2012).

[20] D. G. Dritschel, "Generalized helical Beltrami flows in hydrodynamics and magnetohydrodynamics," J. Fluid Mech. **222**, 525–541 (1991).

[21] M. Jamil and C. Fetecau, "Helical flows of Maxwell fluid between coaxial cylinders with given shear stresses on the boundary," Nonlinear Anal.: Real World Appl. **11**, 4302–4311 (2010).

[22] J.-Z. Wu, H.-Y. Ma, and M.-D. Zhou, *Vorticity and Vortex Dynamics* (Springer Science & Business Media, 2007).

[23] N. H. Ibragimov, *CRC Handbook of Lie Group Analysis of Differential Equations* (CRC Press, 1995), Vol. 2.

[24] V. K. Andreev, O. V. Kaptsov, V. V. Pukhnachev, and A. A. Rodionov, *Applications of Group-Theoretical Methods in Hydrodynamics* (Springer Science & Business Media, 1998), Vol. 450.

[25] S. V. Meleshko and V. V. Pukhnachev, "One class of partially invariant solutions of the Navier-Stokes equations," J. Appl. Mech. Tech. Phys. **40**, 208–216 (1999).

[26] O. Bogoyavlenskij, "Infinite families of exact periodic solutions to the Navier-Stokes equations," Moscow Math. J. **3**, 263–272 (2003).

[27] V. V. Pukhnachev, "Symmetries in the Navier–Stokes equations," Usp. Mekh. **4**, 6–76 (2006).

[28] G. W. Bluman, A. F. Cheviakov, and S. C. Anco, *Applications of Symmetry Methods to Partial Differential Equations* (Springer, 2010).

[29] M. Kumar and R. Kumar, "On some new exact solutions of incompressible steady state Navier-Stokes equations," Meccanica **49**, 335–345 (2014).

[30] H. K. Moffatt, "Helicity and singular structures in fluid dynamics," Proc. Natl. Acad. Sci. U. S. A. **111**, 3663–3670 (2014).

[31] O. Kelbin, A. F. Cheviakov, and M. Oberlack, "New conservation laws of helically symmetric, plane and rotationally symmetric viscous and inviscid flows," J. Fluid Mech. **721**, 340–366 (2013).

[32] D. Dierkes and M. Oberlack, "Euler and Navier-Stokes equations in a new time-dependent helically symmetric system: Derivation of the fundamental system and new conservation laws," J. Fluid Mech. **818**, 344–365 (2017).

[33] P. G. Drazin and N. Riley, *The Navier-Stokes Equations: A Classification of Flows and Exact Solutions* (Cambridge University Press, 2006), Vol. 334.

[34] C. R. Ethier and D. A. Steinman, "Exact fully 3D Navier-Stokes solutions for benchmarking," Int. J. Numer. Methods Fluids **19**, 369–375 (1994).

[35] S. V. Alekseenko, P. A. Kuibin, V. L. Okulov, and S. I. Shtork, "Helical vortices in swirl flow," J. Fluid Mech. **382**, 195–243 (1999).

[36] P. M. Gresho, "Incompressible fluid dynamics: Some fundamental formulation issues," Annu. Rev. Fluid Mech. **23**, 413–453 (1991).

[37] P. Constantin and A. Majda, "The Beltrami spectrum for incompressible fluid flows," Commun. Math. Phys. **115**, 435–456 (1988).

[38] O. I. Bogoyavlenskij, "Exact unsteady solutions to the Navier–Stokes and viscous MHD equations," Phys. Lett. A **307**, 281–286 (2003).

[39] G. I. Taylor, "LXXV. On the decay of vortices in a viscous fluid," London, Edinburgh Dublin Philos. Mag. J. Sci. **46**, 671–674 (1923).

[40] A. Ronveaux, *Heun's Differential Equations* (Oxford University Press, 1995).
[41] G. Kristensson, *Second Order Differential Equations: Special Functions and Their Classification* (Springer Science & Business Media, 2010).
[42] F. M. Arscott, *Heun's Differential Equations* (Clarendon Press, 1995).
[43] A. M. Ishkhanyan and A. E. Grigoryan, "Fifteen classes of solutions of the quantum two-state problem in terms of the confluent Heun function," J. Phys. A: Math. Theor. **47**, 465205 (2014).
[44] L. J. El-Jaick and B. D. B. Figueiredo, "Solutions for confluent and double-confluent Heun equations," J. Math. Phys. **49**, 083508 (2008).
[45] M. Hortaçsu, "Heun functions and their uses in physics," in *Mathematical Physics* (World Scientific, 2013), pp. 23–39.
[46] O. V. Motygin, "On numerical evaluation of the Heun functions," in *2015 Days on Diffraction (DD)* (IEEE, 2015), pp. 1–6.
[47] P. A. Clarkson and M. D. Kruskal, "New similarity reductions of the Boussinesq equation," J. Math. Phys. **30**, 2201–2213 (1989).
[48] K. Kunii, T. Ishida, Y. Duguet, and T. Tsukahara, "Laminar-turbulent coexistence in annular Couette flow," J. Fluid Mech. **879**, 579–603 (2019).
[49] M. Ali and M. Abid, "Self-similar behaviour of a rotor wake vortex core," J. Fluid Mech. **740**, R1 (2014).
[50] C. Selçuk, I. Delbende, and M. Rossi, "Helical vortices: Quasiequilibrium states and their time evolution," Phys. Rev. Fluids **2**, 084701 (2017).
[51] Maplesoft, Maple User Manual, Maplesoft, A Division of Waterloo Maple, Inc., Waterloo, Ontario, 2017.